First Principles Study of Photoelectron Spectra of $\mathrm{Cu}_n{}^-$ Clusters

Carlo Massobrio,[1] Alfredo Pasquarello,[2] and Roberto Car[2,3]
[1]*Institut de Physique Expérimentale, Ecole Polytechnique Fédérale de Lausanne, PHB-Ecublens, CH-1015 Lausanne, Switzerland*
[2]*Institut Romand de Recherche Numérique en Physique des Matériaux (IRRMA), IN-Ecublens, CH-1015 Lausanne, Switzerland*
[3]*Department of Condensed Matter Physics, University of Geneva, CH-1211 Geneva, Switzerland*

(Received 16 December 1994)

We have determined equilibrium geometries and electronic properties of neutral and anionic Cu_n ($n = 2, 9$) clusters by means of first principles calculations in which s and d electrons are treated on equal footing. We find that the calculated electronic density of states is inadequate to interpret photoelectron spectra of $\mathrm{Cu}_n{}^-$ clusters. We obtain good agreement between calculated excitation energies and experimental spectra when we include final states effects.

PACS numbers: 33.80.Eh, 31.15.Ew, 36.40.–c,

Developments in electronic detection techniques have provided in recent years highly resolved photoelectron spectra for a large variety of clusters [1]. The features contained in these spectra convey a wealth of information on the electronic excitation properties and indirectly on the ground state geometries. A reliable interpretation of these spectra is, therefore, a major challenge for theory in the field of clusters, where opportunities for direct comparison with experiments are rare.

So far accurate determination of electronic excitation energies of clusters has been possible only within quantum chemical approaches, such as configuration interaction (CI) schemes [2]. However, due to their prohibitive computational cost, these calculations are limited to clusters containing a very small number of electrons. The increasing amount of spectroscopic data on clusters of different kind calls for a theoretical framework suitable to be extended to more complex systems.

In this context, the case of $\mathrm{Cu}_n{}^-$ clusters constitutes an interesting example of a system containing s and d valence electrons. In early photoelectron spectra, the electron affinities and the onset of the d band have been studied as a function of cluster size [3,4]. The $4s$ band reflects size dependent variations resulting from the delocalized nature of the s electrons, while the $3d$ band evolves monotonically with cluster size. Later, better resolved spectra by Cha, Gantefor, and Eberhardt [5] showed a multitude of distinct features, which could not be discerned previously. These authors have tentatively labeled these spectral features according to the simple shell model. On the theoretical side an interpretation of these spectra has been attempted using an elaborate effective medium theory [6,7]. Although this approach accounted successfully for the relative stability of different clusters [6], it failed in describing satisfactorily the photoelectron spectra [7]. The necessity of treating explicitly a large number of valence electrons has prevented application of CI approaches in $\mathrm{Cu}_n{}^-$ clusters. Thus, a reliable interpretation of these spectra is still lacking.

In this paper, we provide a manageable theoretical scheme which leads to a successful interpretation of the photoelectron spectra of small $\mathrm{Cu}_n{}^-$ clusters. We use a first principles approach based on density functional theory which treats s and d electrons on equal footing. Two factors are crucial to bring theory in close agreement with experiment: first, the accurate determination of the equilibrium atomic geometries of anionic clusters and second, the inclusion of final state effects going beyond a strictly one-electron picture. The importance of s-d hybridization and the limitations of the shell model in both neutral and anionic Cu clusters are shown by an analysis of the electronic wave functions.

We performed calculations within the local density approximation of density functional theory (DF-LDA) by using the method by Car and Parrinello (CP) [8] in conjunction with Vanderbilt ultrasoft pseudopotentials [9]. This approach was already applied successfully to study liquid copper [10] and is described in detail in Ref. [11]. The clusters are placed in a periodic cubic cell of side equal to 25.9 a.u., large enough to avoid interactions of the cluster with its periodic images. The wave functions at the Γ point are expanded in plane waves with an energy cutoff of 15 Ry, whereas the augmented electron density is described with a cutoff of 130 Ry [12]. Exchange and correlation are treated using Perdew and Zunger's interpolation formulas [13]. We have considered anionic $\mathrm{Cu}_n{}^-$ clusters with $n = 3, 5, 7, 9$ [14] and neutral Cu_n clusters with $n = 3, 4, 6, 8$.

Ground state and local minima are found by selecting the initial geometries from those suggested in the literature for Na [15] and Ag [16]. Then we relax the electronic degrees of freedom to their ground state and run repeated cycles of combined steepest descent and CP molecular dynamics. For all neutral clusters we perform an extensive search finding several close local minima by means of a dynamical simulated annealing strategy. Since our structures and energy ordering for neutral Cu clusters are very similar to those found for neutral Ag clusters via configuration interaction (CI) calculations [16], we perform a less extensive search for anionic clusters. In this case we take the CI ground state shapes of $\mathrm{Ag}_n{}^-$ given in Ref. [2] as trial initial structures for local optimization.

0031-9007/95/75(11)/2104(4)$06.00

For Cu_3 our results closely agree with local spin density [17] and CI [18] calculations. In particular, we find for the ground state an obtuse isosceles geometry (apex angle $\alpha = 65.7°$), which is lower by only 0.01 eV than an acute geometry ($\alpha = 56.1°$). Similarly good agreement with Ref. [17] is found for Cu_4. The lowest energy structures for the hexamer are a C_{5v} flat pentagonal pyramid, a truly three-dimensional C_{2v} structure composed of tetrahedral subunits (higher in energy by $\Delta E = 0.01$ eV), and a planar D_{3h} geometry ($\Delta E = 0.04$ eV). A different ordering of these isomers is found for sodium, where the compact C_{2v} structure lies at much higher energy [19]. In the case of Cu_8 the lowest energy isomers are D_{2d} and T_d structures, which are essentially degenerate. These are followed by a capped pentagonal bipyramid (PBP) higher in energy by $\Delta E = 0.20$ eV, and a D_{4d} structure with $\Delta E = 0.5$ eV. Turning to the anionic clusters, we find a linear ground state geometry for Cu_3^-. In the case of Cu_5^- a planar trapezoidal configuration is more stable than the trigonal bipyramid by 0.30 eV. For Cu_7^-, the lowest structure we have obtained is a C_{3v} capped square bipyramid, very close in energy ($\Delta E = 0.01$ eV) to the D_{5h} structure (PBP). The structure found for Cu_9^- is the bicapped PBP of C_2 symmetry. A more detailed account of the structural properties of Cu clusters will be published elsewhere [20].

Electronic properties are first investigated through the electronic density of states (DOS) obtained from the single particle eigenvalues. As a typical example we report in Fig. 1 the DOS of Cu_9^-. We also report on the same figure the atomic s weight of each eigenstate. This has been obtained by projecting the cluster orbitals on the atomic wave functions as described in Ref. [20]. The states in the middle of the band have essentially d character. The states at the band edges have predominantly s character but with a sizable d component due to strong hybridization effects. Similar effects for smaller clusters were observed also in Ref. [17]. The state with less d character is the one at the bottom of the valence band at $E \sim -5.8$ eV.

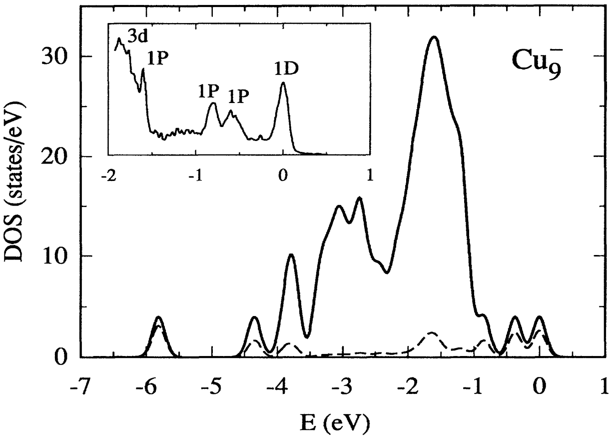

FIG. 1. Calculated density of states for Cu_9^-, convoluted with Gaussians of width 0.1 eV. The dashed line gives the weight of the atomic s character. Inset: experimental photoelectron spectroscopy data of Ref. [5] for Cu_9^-. The Fermi level is at zero energy.

It is of interest to analyze the DOS according to the shell model. To this end, we project the soft part of each eigenfunction, within the Vanderbilt pseudopotential scheme, onto S, P, and D spherical harmonics with respect to the center of mass of the cluster, as detailed in Ref. [15]. This decomposition is displayed in Fig. 2. The case of Cu_9^- corresponds, in the shell model scheme, to a complete filling of the $1S$ and $1P$ levels and to a partial filling of the $1D$ shell with two electrons. Accordingly, since geometrical effects lift the degeneracy of the P level, one would expect to observe in Fig. 2 five main peaks well separated from the d band. As a result of s-d hybridization, we observe instead a more complicated DOS pattern featuring a larger number of peaks with sizable S, P, or D components. As expected, the states in the center of the band, essentially d-like, do not show shell model features, which are present only in states having a substantial atomic s character. Moreover, mixing between S, P, and D spherical components is also observed, in particular, in the highest occupied molecular orbital (HOMO) state.

The inset presented in Fig. 1 allows a direct comparison with the measured photoelectron spectrum of Cu_9^-. Clearly, the three major peaks recorded before the onset of the d band in the experimental data (Fig. 1, inset) are not reproduced by the calculated DOS, which features only two distinct peaks well separated from the d band (Fig. 1). Furthermore, the separation between the HOMO and the first predominant d state is less than 1 eV in the calculated DOS, while in the photoelectron spectrum this separation is larger than 1.5 eV.

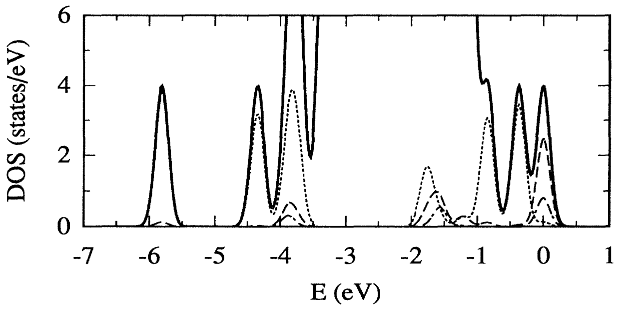

FIG. 2. Decomposition of the DOS for Cu_9^- in angular components S (dash-dotted), P (dotted), and D (dashed). The Fermi level is at zero energy. Note that the state at $E \sim -5.8$ eV is almost completely S. The states in the middle of the band, which do not show shell model features, have atomic d character.

These discrepancies point out the limitations implicit in the interpretation of the photoelectron spectra on the basis of the density of the single-particle eigenvalues. This amounts to neglecting completely the interaction between the hole created by the removal of one electron and the rest of the system [21]. To go beyond this approximation we computed the single-particle excitation energies in terms of differences of self-consistent total energies (ΔSCF) in the context of DF-LDA. In this way, we correct the single-particle eigenvalues for the relaxation shifts resulting from the removal of one electron. This is a meaningful approach provided finite lifetime effects of the hole can be neglected.

We focus on vertical excitation processes; i.e., we keep the atomic geometry unchanged. For every anionic cluster in its ground state geometry we consider all the final states corresponding to the removal of a single electron. These are not ground states and cannot be obtained by a straightforward total energy minimization. Therefore, in order to compute the total energy of the final states we have adopted a constrained minimization procedure in which the hole wave function is frozen. In this way we neglect the relaxation of the hole but we include the screening of the electronic cloud.

The resulting excitation energies for the lowest energy structures, together with the experimental photoelectron spectra, are given in Fig. 3. In the case of Cu$_3^-$ the spectrum exhibits three main features, labeled 1*P*, 1*S*, and 3*d*, the latter indicating the onset of the *d* band and located ~1 eV below the 1*S* split peaks. In our calculation, the uppermost peak has a strong *P* character, while the underlying level is predominantly *S*-like but with a non-negligible *D* component. We notice that the theoretical excitation energies reproduce the main features of the experimental spectrum. This would not be the case if we considered just the calculated DOS in which only one peak, predominantly *P*-like, is well separated from the *d* band. In our calculation we find a single peak associated with the 1*S* feature. This suggests that the origin of the three subpeaks observed experimentally is not *s*-*d* hybridization [5] and could be the result of many-body effects not included in our theory.

For Cu$_5^-$ two major peaks separated by 1.2 eV are discernible in the experimental spectrum, followed by a less distinct feature which immediately precedes the onset of the *d* band. Our result displays two peaks separated by 1.7 eV, the first having a strong *P* character and the second already heavily hybridized with the *d* states. In Ref. [5] the peak at $E \sim -1.7$ eV was taken to correspond to a 1*S* state. Our analysis indicates that a state, almost entirely 1*S*, exists only at the bottom of the band, at $E \sim -5$ eV, suggesting that the *d* band may be closer to the two upper states. Therefore, the experimental feature at $E \sim -1.7$ eV may instead correspond to the small shoulder appearing at $E \sim -2.2$ eV in the calculated excitation energies.

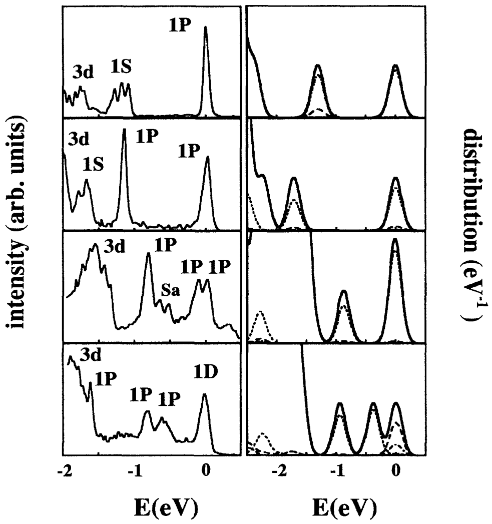

FIG. 3. Comparison between the photoelectron spectra of Ref. [5] (on the left) and our calculated excitation energies (on the right). From top to bottom: Cu$_3^-$, Cu$_5^-$, Cu$_7^-$, Cu$_9^-$. The labeling on the experimental plot is that of Ref. [5] and refers to angular components *S*, *P*, and *D*. Calculated angular components are indicated by dash-dotted (*S*), dotted (*P*), and dashed (*D*) lines. The Fermi level is at zero energy. The calculated distribution of excitation energies has been convoluted with Gaussians of width 0.1 eV.

The data recorded for Cu$_7^-$ are more intriguing and characterized by a split first peak, "satellite" marks related to electronic excitations that follow the photoemission, a second major peak and the underlying *d* band. The main features of this spectrum are in excellent agreement with our calculated results. We find a first peak corresponding to two degenerate states with predominantly *P* character, followed by a second peak resulting from a state also having *P* character but more hybridized with the *d* states. We point out that the calculated excitation energies for the D_{5h} isomer of Cu$_7^-$ also show two peaks above the onset of the *d* band, but it is the second one which originates from degenerate states. Therefore, the C_{3v} structure is in better agreement with experiment that the D_{5h} one, demonstrating that an accurate interpretation of photoelectron experiments can allow one to discriminate between different structural isomers.

For Cu$_9^-$ the calculated excitation energies point towards the existence of three distinct peaks, corresponding well to the three upper features of the experimental data, the first containing a mixed 1*D*-1*S* angular character, the second and the third mostly 1*P*. The steep rising of the *d* band, for energies lower than $E = -1.3$ eV, and the existence of *P*-like states at the bottom of the calculated excitation band suggest that the 1*P* assignment proposed in Ref. [5] at $E \sim 1.5$ eV should instead be considered as a signature of the onset of the *d* band.

Overall the ΔSCF excitation energies are in better agreement with experiment than the single particle eigenvalues. For example, in the case of Cu_9^- the three upper features of the DOS (Fig. 1) are displaced upward and appear well separated from the d band (Fig. 3), when the relaxation shifts are taken into account. This enhancement in the separation between the upper states, which are mostly s-like, and the d band is a common feature of all the clusters considered. Basically states having different localization properties experience different relaxation shifts. This causes the displacement of the d band relative to the upper s states, observed in the calculated excitation energies. These effects are more important for smaller clusters.

Different low-energy isomers can be closer in energy than the LDA accuracy, such as in the case of Cu_7^- where two structures differing by only 0.01 eV are found. As a consequence, identification of ground state structures purely on energetic grounds is not always possible. Furthermore, the clusters observed experimentally are at finite temperature and could be an ensemble of different low-energy isomers. We stress that these considerations do not invalidate our main result, since final state relaxation shifts of the d band relative to the upper s states are qualitatively the same for all clusters in the size range that we have studied. Without inclusion of final state effects, in all cases the number of s-like features above the onset of the d band would be smaller than observed experimentally. This does not exclude that finite temperature effects on the photoelectron spectra could be important. In particular, in some cases, the measured spectra could be a superposition of features belonging to different isomers. Investigation of such effects is an interesting subject for further studies.

In conclusion, we have shown that a scheme based on density functional theory is able to describe accurately photoelectron spectra of complex nanosystems, such as anionic Cu_n^- clusters. The success of our approach rests on a combination of two factors: the determination of the equilibrium structures and the application of a simplified ΔSCF scheme to obtain the excitation energies including final state effects. In particular, this has allowed us to reinterpret previous peak assignments [5] in the photoelectron spectra of Cu_n^- clusters.

Our scheme for excitation energies has to be compared with other methods that treat more accurately many-body effects. For instance, CI calculations have provided successful interpretations of photoelectron spectra, such as in the case of anionic silver clusters [2]. Because of their high computational cost, these calculations are limited to the valence s electrons only and cannot be extended to the case of copper clusters. An alternative method consists in calculating the quasiparticle excitation spectra on the basis of many-body diagrammatic techniques [22]. This approach, which has been used successfully for bulk solids and surfaces, has been applied to metallic clusters only within the spherical jellium model [23]. With respect to both these methods, our scheme has a much lower computational cost and can, therefore, be applied to a wide class of systems.

We acknowledge useful discussions with W. A. de Heer and G. Galli. This work has been partially supported by the Swiss National Science Foundation under Grants No. 20-31240.91 (C. M.) and No. 20.39528.93 (A. P. and R. C.). Most of the calculations were performed on the NEC-SX3 supercomputer of the Swiss Center for Scientific Computing (CSCS).

[1] W. A. de Heer, Rev. Mod. Phys. **65**, 611 (1993).

[2] V. Bonacic-Koutecky *et al.,* J. Chem. Phys. **100**, 490 (1994).

[3] O. Cheshnovsky, K. J. Taylor, J. Conceicao, and R. E. Smalley, Phys. Rev. Lett. **64**, 1785 (1990).

[4] K. J. Taylor, C. L. Pettiette-Hall, O. Cheshnovsky, and R. E. Smalley, J. Chem. Phys. **96**, 3319 (1993).

[5] C. Y. Cha, G. Gantefor, and W. Eberhardt, J. Chem. Phys. **99**, 6308 (1993).

[6] O. B. Christensen, K. W. Jacobsen, J. K. Nørskov, and M. Manninen, Phys. Rev. Lett. **66**, 2219 (1991).

[7] O. B. Christensen, Phys. Rev. B **50**, 1884 (1994).

[8] R. Car and M. Parrinello, Phys. Rev. Lett. **55**, 2471 (1985).

[9] D. Vanderbilt, Phys. Rev. B **41**, 7892 (1990).

[10] A. Pasquarello *et al.,* Phys. Rev. Lett. **69**, 1982 (1992).

[11] K. Laasonen *et al.,* Phys. Rev. B **47**, 10 142 (1993).

[12] With these cutoff values the calculated bonding length ($r_e = 4.11$ a.u.), cohesive energy ($D_e = 3.02$ eV), and vibrational frequency ($\omega_e = 248.8\ \mathrm{cm}^{-1}$) of Cu_2 are not significantly changed with respect to the values $r_e = 4.12$ a.u., $D_e = 3.14$ eV, and $\omega_e = 277.5\ \mathrm{cm}^{-1}$ given in Ref. [10].

[13] J. P. Perdew and A. Zunger, Phys. Rev. B **23**, 5048 (1981).

[14] In the case of anionic clusters, charge neutrality in the periodic cell is preserved by adding a uniform positive background charge.

[15] U. Rothlisberger and W. Andreoni, J. Chem. Phys. **94**, 8129 (1991).

[16] V. Bonacic-Koutecky *et al.,* J. Chem. Phys. **98**, 7981 (1993).

[17] K. A. Jackson, Phys. Rev. B **47**, 9715 (1993).

[18] S. R. Langhoff, C. W. Bauschlicher, S. P. Walch, and B. C. Laskowski, J. Chem. Phys. **85**, 7211 (1986).

[19] V. Bonacic-Koutecky *et al.,* J. Chem. Phys. **96**, 7938 (1992).

[20] C. Massobrio, A. Pasquarello, and R. Car (to be published).

[21] G. Wendin, *Breakdown of the One-electron Picture in Photoelectron Spectra,* Structure and Bonding Vol. 45 (Springer, Berlin, Heidelberg, 1981).

[22] M. S. Hybertsen and S. G. Louie, Phys. Rev. Lett. **55**, 1418 (1985); Phys. Rev. B **34**, 5390 (1986).

[23] S. Saito, S. B. Zhang, S. G. Louie, and M. L. Cohen, Phys. Rev. B **40**, 3643 (1989).